First principles study of Structural, Electronic and Mechanical properties of TiN and TiN$_2$

R.Rajeswarapalanichamy[a*], G. Sudhapriyanga[a], R. Murugeswari[a], M. Kavitha[a], M.Santhosh[a], K. Iyakutti[c]

Abstract: The structural, electronic and mechanical properties of TiN and TiN$_2$ are investigated using density functional theory calculations with the generalized gradient (GGA) approximation. The lattice constants, cohesive energy, bulk modulus and the density of states are obtained. The calculated lattice parameters are in good agreement with the available results. The electronic structure reveals that these materials exhibit metallic behavior at ambient condition. A pressure-induced structural phase transition from NaCl to ZB to WZ phase is observed in TiN whereas in TiN$_2$, CaF$_2$ to FeS$_2$ to AlB$_2$ transition is predicted. The computed elastic constants indicate that these nitrides are mechanically stable at ambient pressure.

Keywords— Ab-initio calculations, Electronic structure, Structural phase transition, Elastic properties.

———————————— ◆ ————————————

1 INTRODUCTION

Recently, titanium nitride has attractive interests because of its simple structure and special properties such as high melting point, high hardness, high corrosion resistance, high specific strength, and high conductivity. TiN has been mainly applied in hard coatings [1] due to its exceptional combination of physical properties and chemical and metallurgical stability [2]. Many experimental and theoretical studies have been focused on the structural, mechanical, electronic, and optical properties of TiN [3-5]. Fernindez Guillermet et.al investigated the cohesive properties of 4d-transition-metal nitrides in the NaC1-type structure [6]. Grossman et.al [7] studied the trends in electronic and structural properties of TiN by ab-initio computational method. Stampfl et.al [8] investigated the electronic structure and physical properties of TiN using density functional theory.

To the best of our knowledge, the structural, electronic and elastic properties of TiN$_2$ are not yet reported. In the present paper, Structural, electronic and elastic properties of TiN and TiN$_2$ are investigated using VASP code.

2 COMPUTATIONAL DETAILS

The total energy calculations are performed in the frame work of density functional theory using the generalized gradient approximation (GGA-PBE) as implemented in the VASP code [9]. Ground state geometries are determined by minimizing stresses and Hellman-Feynman forces using the conjugate-gradient algorithm with force convergence less than 10^{-3} eV Å^{-1} and the Brillouin zone integration is performed with a Gaussian broadening of 0.1 eV. The cutoff energy for plane waves in our calculation is 400eV. The valence electronic configurations are Ti 3d^2 4s^2 and N 2s^2 2p^3 atoms. Brillouin zone integrations are performed on the Monkhorst-Pack K-point mesh with a grid size of 12x12x12 (TiN) and 8x8x8 (TiN$_2$) for structural optimization and the total energy calculation.

3 RESULTS AND DISCUSSION

3.1 Structural Properties

The structural stability of TiN and TiN$_2$ is analyzed by calculating the total energy using VASP code based on density functional theory. The calculated ground state properties like lattice constants a,c (Å), cell volume V_0 (Å^3), valence electron density ρ(electrons/ Å^3), cohesive energy (eV), bulk modulus B_0 (GPa) and its derivative B_0' for TiN and TiN$_2$ with considered phases are listed in Table 1 and is compared with the experimental [10-12] and other available theoretical data [13-17]. From Table 1, it is found that the calculated equilibrium lattice constant and bulk modulus are in good agreement with the experimental and other available theoretical results. It is also observed that, for TiN, cubic-NaCl phase owing to its highest cohesive energy, it is the most stable one among the considered phases. For TiN$_2$, it is found that, CaF$_2$ phase is the most stable one. The total energy vs reduced volume plot for TiN and TiN$_2$ is given in Fig.1 (a-b) respectively. From Fig.1 (a-b), it is noted that TiN is stable in NaCl phase, whereas TiN$_2$ is stable in CaF$_2$ phase. On further reducing the volume, a sequence of structural phase transition occurs from NaCl→ZB→WZ in TiN and CaF$_2$→FeS$_2$→AlB$_2$ in TiN$_2$.

In order to determine transition pressure, the enthalpy is calculated using the formula

H=E+PV

————————————————

[a]*Department of Physics, N.M.S.S.V.N college, Madurai, Tamilnadu-625019, India*

[c]*Department of Physics & Nanotechnology, SRM University, Chennai, Tamilnadu-603203. India.*

Corresponding author E-mail: *rrpalanichamy@gmail.com*

TABLE 1
CALCULATED LATTICE PARAMETERS A,C (Å), VALENCE ELECTRON DENSITY VED (ELECTRONS/ Å^3), COHESIVE ENERGY E_{COH} (EV) BULK MODULUS B_0 AND ITS DERIVATIVE B_0' FOR THE TiN AND TiN$_2$ FOR POSSIBLE STRUCTURES.

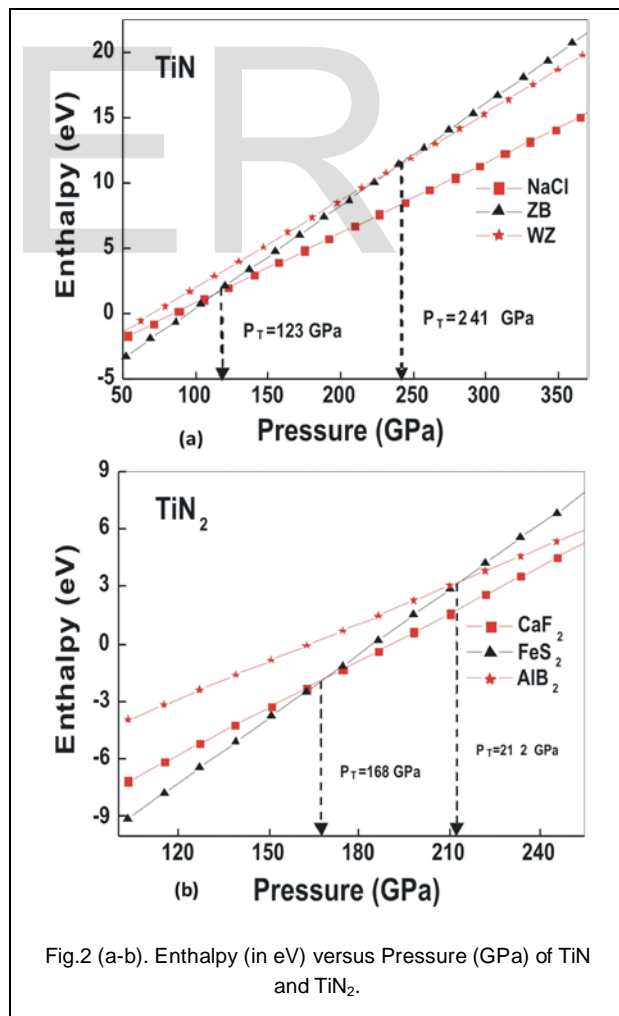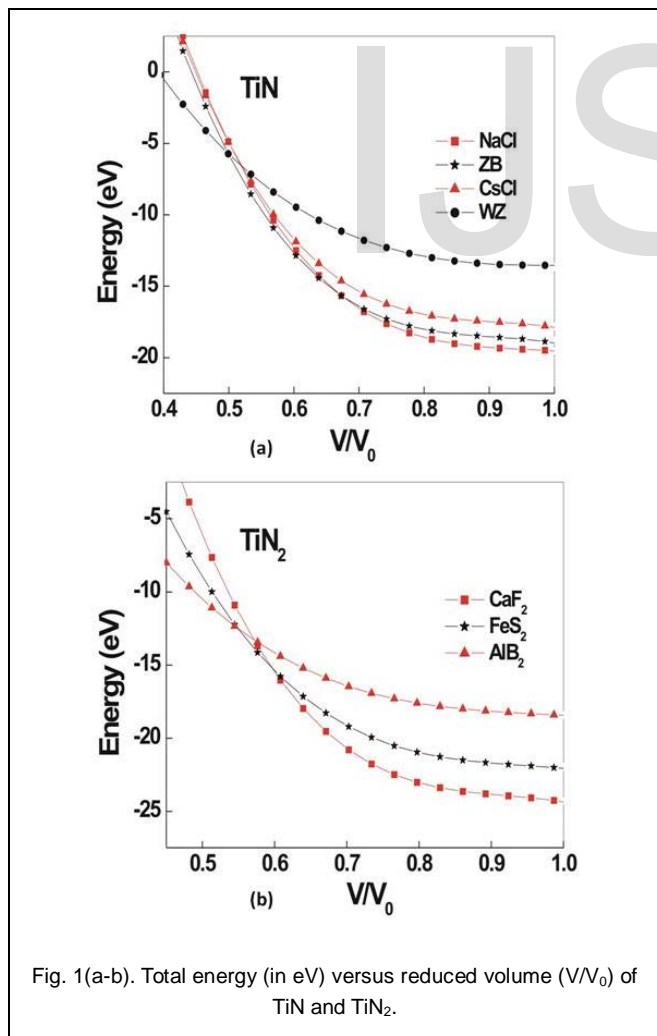|	TiN				TiN$_2$		
	NaCl	CsCl	ZB	WZ	CaF2	FeS2	AlB2
a	4.259 4.25 [10] 4.241[11] 4.24 [12] 4.251[13] 4.26 [14] 4.247[15] 4.261[16]	2.637	4.62	2.555	4.912	3.85	2.888
c				4.215			4.7652
V_0	19.313	21.38	24.51	23.97	29.63	28.53	34.15
VED	0.465	0.420	0.367	0.376	0.472	0.491	0.409
E_{coh}	13.3304	11.646	12.434	7.368	17.090	14.8245	11.2154
B_0	308 320[17]	305	306	287	181	142	177
B_0'	4.98	4.88	4.61	4.52	4.10	3.92	3.95

Fig. 1(a-b). Total energy (in eV) versus reduced volume (V/V$_0$) of TiN and TiN$_2$.

Fig.2 (a-b). Enthalpy (in eV) versus Pressure (GPa) of TiN and TiN$_2$.

The transition pressure (P_T) value is determined from the intersection of enthalpy versus pressure curve and is presented in Fig. 2 (a-b). For TiN, it is found that the transition pressure for NaCl to ZB is 123 GPa and ZB to WZ is 241 GPa. In TiN_2, P_T value for CaF_2 to FeS_2 transition is 168 GPa and FeS_2 to AlB_2 is 212 GPa.

3.2 Electronic Properties

The total density of states (DOS) of TiN and TiN_2 at normal pressure are shown in Fig.3 (a-b). The peak due to 2s state electrons of the nitrogen atom present at the energy range of ~ -10eV for TiN, doubles for TiN_2 due to two nitrogen atoms. The d state electrons of the Ti atom and the N-2p state electrons contribute to the highest spike just below the Fermi level, indicating that the Ti-d states intensively hybridize with the N-2p states. Above the Fermi level the peaks are due to Ti-p, Ti-d states and N-d states.
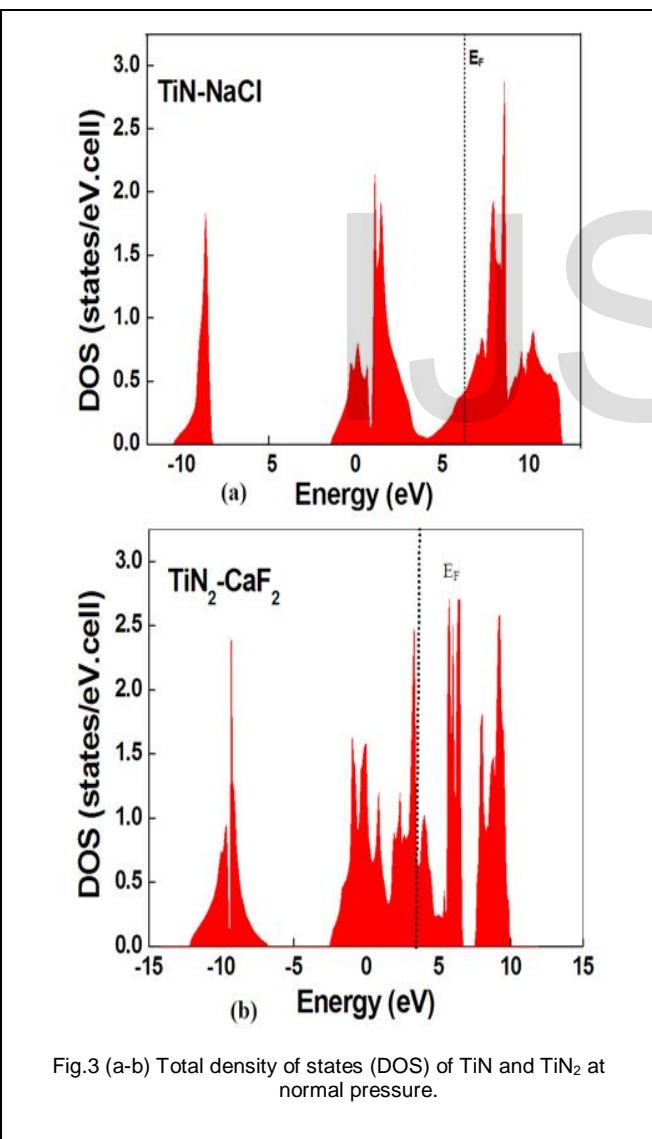

Fig.3 (a-b) Total density of states (DOS) of TiN and TiN_2 at normal pressure.

The covalent characteristics between titanium and N atoms can be confirmed by the charge density distribution. The charge density distribution for TiN and TiN_2 at normal pressure is shown in Figure 4(a-b). It is clearly seen that charge strongly accumulates between Ti and N atoms, which means that a strong directional bonding exists between them. The bonding nature of these materials is found to be covalent-like due to the hybridization of N and Ti atoms, but there is also some ionic character with electron transfer from the titanium to nitrogen atoms. Thus, our results demonstrate that the bonding is a mixture of covalent and ionic attribution.
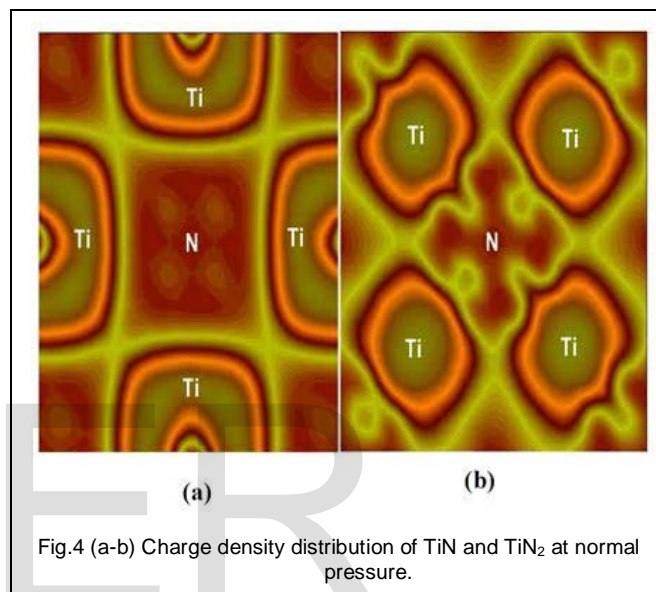

Fig.4 (a-b) Charge density distribution of TiN and TiN_2 at normal pressure.

3.3 Elastic Properties

In order to calculate the elastic constants of a structure, a small strain is applied on to the structure and its stress is determined. The energy of a strained system [18] can be expressed in terms of the elastic constants C_{ij} as:

$$\Delta E = \frac{E(\{e_i\}) - E_0}{V_0} = \left(1 - \frac{V}{V_0}\right) P(V_0) + \frac{1}{2}\left(\sum_1^6 \sum_1^6 C_{ij} e_i e_j\right) + O(\{e_i^3\})$$

where V_0 is the volume of the unstrained lattice, E_0 is the total minimum energy at this unstrained volume of the crystal, $P(V_0)$ is the pressure of the unstrained lattice, and V is the new volume of the lattice due to strain tensor. The elasticity tensor has three independent components (C_{11}, C_{12}, C_{44}) for cubic crystals and five (C_{11}, C_{12}, C_{44}, C_{13}, C_{33}) for hexagonal crystals. The calculated elastic constants C_{ij}(GPa), Young's modulus E(GPa), shear modulus G(GPa), and Poisson's ratio (v) are presented in Table 2. From tabulated values, it is found that the calculated elastic constants are in agreement with the experimental [19, 20] and other available theoretical data [21, 6]. For a stable cubic structure, the three independent elastic constants C_{ij} (C_{11}, C_{12}, C_{44}) should satisfy the Born-Huang criteria for the stability of cubic crystals [22]. It is seen that, the calculated elastic constants of TiN and TiN_2 satisfy Born-Huang

TABLE 2

CALCULATED ELASTIC CONSTANTS C_{11}, C_{12}, C_{44} (GPA), YOUNG'S MODULUS E (GPA), SHEAR MODULUS G(GPA),
B/G RATIO, ANISOTROPIC FACTOR AND (A) POISSON'S RATIO FOR THE TiN AND TiN$_2$ FOR STABLE PHASE.

	C_{11}	C_{12}	C_{44}	E	G	ν	B/G	A
TiN	568	179	109	371	143	0.298	2.15	0.56
	631[19, 20]	171 [19, 20]	170 [19, 20]					
	598 [21]	154 [21]	168 [21]					
	610 [6]	100 [6]	168 [6]					
TiN$_2$	248	98	106	239	94	0.278	1.92	1.41

criteria, suggesting that they are mechanically stable. The young's modulus [23] is higher for TiN than TiN$_2$. Hence, TiN is the stiffer than TiN$_2$.

4 CONCLUSION

The structural, electronic and elastic properties of TiN and TiN$_2$ are investigated. The computed equilibrium lattice parameters and bulk modulus values are consistent with the experimental and other available theoretical results. TiN is found to be stable in the NaCl phase whereas TiN$_2$ is stable in CaF$_2$ phase at ambient pressure. A sequence of pressure-induced structural phase transition occurs from NaCl→ZB→WZ in TiN and CaF$_2$→FeS$_2$→AlB$_2$. The density of states of TiN and TiN$_2$ confirm their metallic nature. The calculated elastic constants obey the necessary mechanical stability conditions suggesting that they are mechanically stable at ambient pressure and TiN is found to be the hardest material.

ACKNOWLEDGMENT

REFERENCES

[1] H.E. Rebenne and D.G. Bhat, Surf. Coat. Technol, 63 (1994) 1.

[2] K. Schwarz, CRC Crit. Rev. Solid State Mater. Sci. 13 (1987) 211.

[3] H. Hochst, R.D. Bringans, P.Steiner and T.Wolf, Phys.Rev. B 25 (1982) 7183.

[4] Z. Dridi, B. Bouhafs, P. Ruterana, and H. Aourag, J. Phys.: Condense. Matter 14 (2002) 10237.

[5] M. Guemmaz, G. Moraitis, A. Mossar, M.A. Khan, and J.C.Parlebas, J. Phys.: Condense. Matter 9 (1997) 8453.

[6] A. Fernindez Guillermet, Phys.Rev. B 45 (1992) 11557.

[7] Jeffery C.Grossman, Ari Mizel, Michale Cote, L.Cohen, and Steven G.Louie. Phys.Rev. B 60 (1999) 6343.

[8] C. Stampfl, W.Mannstadt, R.Aashi, and A.J.Freeman, Phys.Rev. B 63 (2001) 155106.

[9] G. Kresse, J. Furthmuller, Comput. Mater. Sci. 6 (1996) 15.

[10] J.O.Kim, J.D.Achenbach, P.B. Mirkarimi, M. Shinn and S.A. Barnett, J.Appl. Phys 72 (1992) 1805.

[11] E.K. Storms, The Refractory Carbides, Academic press, Newyork, 1967.

[12] S.F. Pugh, Philos. Mag. 45 (1954) 823.

[13] R.Ahuja, O. Eriksson, J.M. Wills and B. Johansson, Phys. Rev B 53 (1996).

[14] V. Richet, A.Beger, J.Drobniewski, I.Endle, E.Wolf, Mater. Sci. Eng.A 209 (1996) 353.

[15] W. Feng, S.Cui, H.Hu, G.Zhang, Z.Lu, Physica B 406 (2011) 3631.

[16] W.Wolf, R. Podloucky, T. Antretter, and F.D. Fisher, Philos.Mag. B 79 (1999) 839.

[17] R.W.G. Wyckoff, Crystal structures, 2nd ed. (Wiley, Newyork, 1963) vol-1, p.86.

[18] J. F. Nye, Physical Properties of Crystals, Oxford University Press, Oxford (1985).

[19] W.Weber, Phys. Rev. B 8 (1973) 5082.

[20] V.P. Zhukov, V.A. Gubanov, O. Jepson, N.E. Christensen, O.K. Anderson, J. Phys. Chem. Solids, 49 (1988) 841.

[21] A. Zaoui, B. Bouhafs, P. Ruterana, Mater. Chem. Phys. 91 (2005) 108.

[22] M. Born, K. Huang, Dynamical Theory of Crystal Lattices, Clarendon, Oxford, (1956).

[23] K. A. Matori, M. H. M. Zaid, H. A. A. Sidek, M. K. Halimah, Z. A. Wahab and M. G. M. Sabri, Int. J.Physical Sciences. 5(2010) 2212-2216.